



## OPEN ACCESS

## EDITED BY

Delphine Le Roux,  
UMR BIPAR (Anses, EnvA, INRAE) École  
Nationale Vétérinaire d'Alfort, France

## REVIEWED BY

Yasuhiro Takashima,  
Gifu University, Japan  
Vitomir Djokic,  
Environmental and Occupational  
Health & Safety (ANSES), France  
Marie France Cesbron-Delauw,  
Centre National de la Recherche  
Scientifique (CNRS), France

## \*CORRESPONDENCE

Antonio Barragan  
antonio.barragan@su.se

## SPECIALTY SECTION

This article was submitted to  
Parasite Immunology,  
a section of the journal  
Frontiers in Immunology

RECEIVED 23 May 2022

ACCEPTED 12 July 2022

PUBLISHED 03 August 2022

## CITATION

Ross EC, Hoeve ALT, Saeij JPJ and  
Barragan A (2022) *Toxoplasma*  
effector-induced ICAM-1 expression  
by infected dendritic cells potentiates  
transmigration across  
polarised endothelium.  
*Front. Immunol.* 13:950914.  
doi: 10.3389/fimmu.2022.950914

## COPYRIGHT

© 2022 Ross, Hoeve, Saeij and  
Barragan. This is an open-access article  
distributed under the terms of the  
[Creative Commons Attribution License  
\(CC BY\)](https://creativecommons.org/licenses/by/4.0/). The use, distribution or  
reproduction in other forums is  
permitted, provided the original  
author(s) and the copyright owner(s)  
are credited and that the original  
publication in this journal is cited, in  
accordance with accepted academic  
practice. No use, distribution or  
reproduction is permitted which does  
not comply with these terms.

# *Toxoplasma* effector-induced ICAM-1 expression by infected dendritic cells potentiates transmigration across polarised endothelium

Emily C. Ross<sup>1</sup>, Arne L. ten Hoeve<sup>1</sup>, Jeroen P. J. Saeij<sup>2</sup>  
and Antonio Barragan<sup>1\*</sup>

<sup>1</sup>Department of Molecular Biosciences, The Wenner-Gren Institute, Stockholm University, Stockholm, Sweden, <sup>2</sup>Department of Pathology, Microbiology, and Immunology, University of California, Davis, Davis, CA, United States

The obligate intracellular parasite *Toxoplasma gondii* makes use of infected leukocytes for systemic dissemination. Yet, how infection impacts the processes of leukocyte diapedesis has remained unresolved. Here, we addressed the effects of *T. gondii* infection on the trans-endothelial migration (TEM) of dendritic cells (DCs) across polarised brain endothelial monolayers. We report that upregulated expression of leukocyte ICAM-1 is a feature of the enhanced TEM of parasitised DCs. The secreted parasite effector GRA15 induced an elevated expression of ICAM-1 in infected DCs that was associated with enhanced cell adhesion and TEM. Consequently, gene silencing of *Icam-1* in primary DCs or deletion of parasite GRA15 reduced TEM. Further, the parasite effector TgWIP, which impacts the regulation of host actin dynamics, facilitated TEM across polarised endothelium. The data highlight that the concerted action of the secreted effectors GRA15 and TgWIP modulate the leukocyte-endothelial interactions of TEM in a parasite genotype-related fashion to promote dissemination. In addition to the canonical roles of endothelial ICAM-1, this study identifies a previously unappreciated role for leukocyte ICAM-1 in infection-related TEM.

## KEYWORDS

leukocyte, blood-brain barrier, apicomplexa, trans-endothelial migration, cell adhesion molecule (CAM), immune cell

## Introduction

The blood-brain barrier (BBB) separates the blood from the brain parenchyma. In the neurovascular unit, the endothelium regulates and heavily restricts the movement of molecules, cells and pathogens between the two compartments (1). Yet, leukocytes can enter the brain parenchyma in a tightly regulated fashion, which is crucial to resolve infection or other insults. Paradoxically, leukocytes can also be utilized by pathogens to gain access to the brain (2).

The process of leukocyte trans-endothelial migration (TEM), also termed diapedesis, entails signalling cascades (3) and a tight interplay of leukocytes with the endothelium (4). In the leukocyte's approach to the site of TEM, crucial interactions between intercellular cell adhesion molecule-1 (ICAM-1) on the endothelium and leukocyte integrins, such as LFA-1 ( $\alpha_1\beta_2$ ; CD11a/CD18), precede translocation (5, 6). However, while most leukocyte subsets express ICAM-1, the putative role of leukocyte ICAM-1 in diapedesis has remained unresolved (7, 8). Intracellular microbes hijack host cell functions and, therefore, the study of host-pathogen interactions can provide unique cues on the biology of leukocyte migration.

The obligate intracellular parasite *Toxoplasma gondii* chronically infects a significant portion of the global human population and warm-blooded vertebrates (9). Reactivated infection in immunocompromised individuals or congenital infection in the developing foetus can result in severe neurological manifestations (10). Yet, primary infection is often asymptomatic or accompanied by mild flu-like symptomatology (10). This implies that early passage to the central nervous system is generally clinically silent and yields chronic, possibly life-long, latent infection (11, 12). In Europe and North America, three clonal lineages of *T. gondii* prevail (type I, II, III), with type II strains being commonly carried by humans and by animals used for meat consumption (13, 14).

*T. gondii* actively infects nucleated cells, including immune cells. Parasitised dendritic cells (DCs) and other mononuclear phagocytes mediate systemic dissemination of *T. gondii* (15, 16). Passage of *T. gondii* to the brain parenchyma is restricted by the BBB (17) and alternative translocation pathways, including trafficking inside leukocytes, have been proposed (12, 18). Secretory rhoptry organelles are discharged upon host cell invasion and once the parasite resides in its intracellular niche, the parasitophorous vacuole (PV), dense granules contents are discharged. Notably, effector proteins from these two secretory compartments impact host cell transcription and signalling, and thus the host-parasite interaction (19, 20). The effector protein TgWIP is secreted from rhoptries into the host cytosol and impacts the migration of parasitised DCs across transwell filters (21). In addition, a number of dense granule proteins (GRA) are transported across the PV into the host cell cytosol, which is dependent on Myc regulation proteins (MYR). In contrast, the

effector functions of the polymorphic effector protein GRA15, which is inserted into the PV membrane, do not depend on MYR (22). GRA15 from type II *T. gondii* strains activates the NF $\kappa$ B pathway, leading to macrophage production of inflammatory cytokines (23).

We recently described an important role for leukocyte integrins and endothelial CAMs in the transmigration of *T. gondii*-challenged DCs across polarised monolayers of primary murine brain endothelium (24). However, while endothelial ICAM-1 is crucial for TEM (4), the implication of leukocyte ICAM-1 in diapedesis and, specifically, in TEM associated with microbial pathogenesis has remained unexplored (25). Here, we describe a role for *T. gondii* effector-induced leukocyte ICAM-1 in TEM and provide a framework for further exploration of the described differences between *T. gondii* lineages in transmigration *in vitro* and systemic dissemination in mice (26).

## Materials and methods

### Ethics statement

The Regional Animal Research Ethical Board, Stockholm, Sweden, approved protocols involving extraction of cells from mice, following proceedings described in EU legislation (Council Directive 2010/63/EU).

### Parasite culture and cell lines

*T. gondii* type I (RH) and II (ME49, PRU) strains and mutant lines ( $\Delta$ MYR1,  $\Delta$ TgWIP,  $\Delta$ GRA15) are detailed in [Supplementary Table 1](#) and were maintained by serial 48 h passaging in human foreskin fibroblasts (HFF; CRL-2088, American Type Culture Collection). HFF and mouse brain endothelial cells (bEnd.3, CRL-2299, American Type Culture Collection) were cultured in Dulbecco's modified Eagle's medium (DMEM, ThermoFisher scientific) with 10% heat inactivated foetal bovine serum (FBS, Sigma), gentamicin (20  $\mu$ g/ml, Gibco), L-glutamine (2 mM, Gibco) and HEPES (10 mM, Gibco). Cell cultures and parasites were grown in a humidified atmosphere containing 5% CO<sub>2</sub> at 37°C and regularly tested for *Mycoplasma*.

### Primary DCs

Murine bone marrow-derived DCs were generated as previously described (27). Briefly, cells from bone marrow of 6-10 week old male or female C57BL/6Ncrl mice (Charles River) were cultivated in RPMI 1640 with 10% FBS,

gentamicin (20 µg/ml), glutamine (2mM) and HEPES (0.01 M), referred to as complete medium (CM), and supplemented with 10 ng/ml recombinant mouse GM-CSF (Peprotech). Loosely adherent cells (DCs) were harvested after 6 or 8 days of maturation.

## Polarisation parameters: Permeability assay and transendothelial electrical resistance (TEER)

bEnd.3 cells were cultured to 80% confluence then seeded onto transwells (8 µm pore size; BD Biosciences) and grown for 5 d until they reached polarisation, as defined below. For evaluation of cell monolayer permeability following transmigration, FITC-dextran (3 kDa; Life tech) was added to the upper compartment of the transwell at a concentration of 12.5 µg/ml for 90 min. Medium was collected from the lower compartment, and fluorescence was measured in a fluorometer (EnSpire Multimode Plate Reader, Perkin Elmer) at 485 nm excitation 520 nm emission. Fluorescence intensity was measured as arbitrary fluorescence units (a.u.) at a sensitivity of < 1 fmol fluorescein/well, as specified by the manufacturer. Polarised monolayers were defined by a TEER  $\geq 250 \Omega \cdot \text{cm}^2$ , as measured using an Ohmmeter (Millipore, Bedford, MA) and correcting measurements with the formula: Unit Area Resistance (TEER) = Resistance ( $\Omega$ ) \* Effective Membrane Area ( $\text{cm}^2$ ). TEER was measured before and after transmigration or treatments. Values are shown as percentage (%) of TEER related to TEER prior to treatments or transmigration.

## Motility and transmigration assays

Motility assays were performed as previously described (24). Briefly, DCs were challenged with freshly egressed *T. gondii* tachyzoites (MOI 3) for 4 h (resulting in 70–80% infection frequency) and with soluble reagents as indicated. DCs were then added to 96-well plates pre-cultured with bEnd.3 cells. Live cell imaging was performed for 1 h, 1 frame/min, at 10X magnification (Z1 Observer with Zen 2 Blue v. 4.0.3, Zeiss). Time-lapse images were consolidated into stacks and motility data was obtained from 30 cells/condition (Manual Tracking, ImageJ) yielding mean velocities (Chemotaxis and migration tool, v. 2.0). Infected cells were defined by GFP<sup>+</sup> or RFP<sup>+</sup> cells, as indicated.

Transmigration assays were performed as previously described (24). Briefly, DCs were cultured with CM  $\pm$  freshly egressed *T. gondii* tachyzoites (MOI 2, 4 h) and then transferred to transwells with pre-cultured bEnd.3 monolayers. After 16 h, transmigrated DCs were put on ice for 1 h to disassociate adherent cells, and then counted manually in a Bürker chamber by light microscopy. For each independent

experiment, duplicate or triplicate technical replicates were assessed and means calculated.

## Motility assays under shear stress

Flow motility assays were performed as previously described (24). Briefly, DCs were challenged as stated under motility assay and then added to fluidic channels ( $\mu$ -Slide VI0.4; Ibidi) with confluent bEnd.3 cell monolayers and allowed to adhere for 10 min. Phase-contrast and fluorescence images were first captured in static condition. Fluidic shear stress was then applied by flowing CM at 0.2 dyn/cm<sup>2</sup> through the channels. Live cell imaging was immediately initiated and images acquired every 10 s for up to 10 min, at 10X magnification (Z1 Observer with Zen 2 Blue v. 4.0.3, Zeiss). Time-lapse images were consolidated into stacks and motility and path-length data obtained from 20–30 cells (Manual Tracking, ImageJ) yielding individual cell velocities and pathlengths (Chemotaxis and migration tool, v 0.2.0).

## Flow cytometry

Bone marrow-derived DCs were cultured in CM  $\pm$  freshly egressed *T. gondii* tachyzoites (MOI 1) for 24 h. Cells were stained on ice in FACS buffer (1% FBS and 1 mM EDTA in PBS) with Live/Dead Violet (L34955, Life technologies), anti-mouse CD11c PE-Cy7 (clone N418, 25-0144-82, eBioscience) and anti-mouse CD18 PE (clone M18/2, 101407, BioLegend) or anti-mouse CD29 Alexa Fluor 647 (clone HM $\beta$ 1-1, 102213, BioLegend) or anti-mouse CD54 APC (clone YN1/1.7.4, 116119, BioLegend) or IgG2a PE isotype control (clone R35-95, 553930, BD Pharmingen) antibodies, fixed with 2% PFA and acquired on a BD LSRFortessa flow cytometer (BD Biosciences). The results were then analysed with FlowJo software (v. 10, FlowJo LLC). Prior to staining, cells were blocked in FACS buffer supplemented with the Fc blocking anti-mouse CD16/CD32 antibody (clone 93, 14-0161-82, eBioscience). Infected cells were defined as GFP<sup>+</sup> cells when challenged with GFP-expressing *T. gondii*. For *T. gondii* strains that lack a fluorescent reporter (PRU $\Delta$ ku80 and PRU $\Delta$ MYR1, Supplementary Figure 1D), cells were permeabilized with 1% Triton X-100 in FACS buffer and stained with primary mouse anti-*T. gondii* SAG1 (clone P30/3, MA1-83499, ThermoFisher) and chicken anti-mouse IgG (H+L) Alexa Fluor 488-conjugated (A-21200, ThermoFisher) secondary antibodies. Infected cells were then defined as Alexa Fluor 488<sup>+</sup>.

## Immunostainings

Unchallenged or *T. gondii*-challenged DCs were plated on coverslips pre-coated with 1% gelatin (BioRad). Cells were fixed

(4% PFA, Sigma-Aldrich), blocked (5% FBS in PBS for 2 h), then incubated with rat anti-mouse CD54 (ICAM-1; clone YN1/1.7.4; eBioscience) at 1:200 overnight at 4°C. Cells were then stained with chicken anti-rat IgG (H+L) Alexa Fluor 594-conjugated secondary antibody (1:1000) and DAPI for 2 h, mounted and imaged using a 63X objective (DMi8, Leica Microsystems). The ICAM-1 signal intensity of *T. gondii*-infected cells (GFP<sup>+</sup>) and by-stander cells (GFP<sup>-</sup>) from randomly chosen fields of view (4–5/per condition and experiment) was measured in ImageJ, and corrected for with the following formula; Integrated Density – (Area of selected cell X Mean fluorescence of background readings). The corrected value is shown in graphs as arbitrary units (a.u.). For live imaging, *T. gondii*-challenged DCs were blocked with anti-CD16/CD32 antibody (clone 93, 14-0161-82, eBioscience), stained with anti-mouse CD54-APC (clone YN1/1.7.4, 116119, BioLegend) antibody on ice, washed, seeded on bEnd.3 cells and imaged for 1 h.

## Lentiviral vector production and *in vitro* transduction

A self-complementary hairpin DNA oligo targeting *Icam1* (shICAM1, TRCN0000218257, Genscript) mRNA was on self-inactivating lentiviral vectors (pLL3.7) with eGFP reporter expression (Supplementary Table 2). Transfer plasmid (shRNA targeting *Icam1* or *Luc*) was co-transfected with psPAX2 (12260, Addgene) packaging vector and pCMV-VSVg (8454, Addgene) envelope vector into Lenti-X 293 T cells (Clontech) using Lipofectamine 2000 (Invitrogen). The resulting supernatant was harvested 24 h and 48 h post-transfection. Supernatants were centrifuged to eliminate cell debris and filtered through 0.45-mm cellulose acetate filters. DCs (5 days post-bone marrow extraction) were transduced by adding lentiviral supernatants in the presence of DEAE dextran (8 µg/ml; Sigma-Aldrich) to cells for 4 h. After 2–3 days (7–8 days post-bone marrow extraction), transduction efficiency was examined for eGFP expression by epifluorescence microscopy (Z1 Observer with Zen 2 Blue v. 4.0.3, Zeiss) followed by expression analysis by qPCR for knock-down of targeted mRNA.

## Polymerase chain reaction (PCR)

Total RNA was extracted using TRIzol reagent (Sigma-Aldrich). First-strand cDNA was synthesised with Maxima H Minus Reverse Transcriptase (Thermo Fisher). Real-time quantitative polymerase chain reaction (qPCR) was performed using SYBR green PCR master mix (Kapa biosystems), forward and reverse primers (200 nM), and cDNA (100 ng) with a QuantStudio<sup>TM</sup> 5 real-time PCR system (ThermoFisher). Glyceraldehyde 3-phosphate dehydrogenase (GAPDH) was used as a house-keeping gene to generate  $\Delta$ Ct values; 2<sup>– $\Delta$ Ct</sup> values were used to calculate relative expression. All primers (Invitrogen) were designed using the Get-prime or Primer-BLAST software (Supplementary Table 3).

## Statistical analyses

All statistics were performed with Prism software (v. 8, GraphPad). Multiple comparisons were carried out by one-way ANOVA, Sidak's *post-hoc* test, while 2-sample tests were conducted with a Student's t-test on normally distributed sample populations. A *p*-value less than 0.05 was considered to be statistically significant. All data are from 3 or more biological replicates separated in time.

## Results

### Parasite effectors impact the transmigration frequency of parasitised DCs across polarised endothelial cell monolayers in a genotype-related fashion

Previous studies established that *T. gondii*-infected DCs perform TEM across polarised endothelial cell monolayers at a higher frequency than unchallenged DCs (24) and that the shuttling function of DCs in mice is related to the parasite genotype (26). To assess whether TEM is genotype-dependent, DCs infected with a type I prototypic strain (RH) or type II strain (ME49) were assessed for transmigration across polarised endothelium (bEnd.3). While both genotypes induced TEM, the type II strain consistently induced superior transmigration frequencies (Figure 1A), at comparable infection frequencies (Supplementary Figure 1A). As previously described (24), transmigration of *T. gondii*-challenged DCs occurred in the absence of elevated permeability to the low-molecular weight tracer FITC-dextran and with maintained TEER (Figures 1B, C), indicating preserved cellular barrier integrity.

Because rolling, arrest and crawling are steps that precede the transmigration of leukocytes across endothelium (28), next, we assessed the migratory behaviour of infected DCs on endothelium. Interestingly, while type II-infected DCs exhibited superior transmigration frequency compared to type I-infected DCs (Figure 1A), type I-infected DCs, but not type II-infected DCs, exhibited an elevated motility on endothelium (Figure 1D). These relative but consistent strain-related phenotypical differences motivated an exploration of strain-related effectors. First, we confirmed that the rhoptry effector TgWIP impacted transmigration for type II-infected DCs (21). However, because the elevation of transmigration was only partially reduced upon TgWIP deletion (Figure 1E), we hypothesized that additional secretory pathways were in play. Challenge with parasite mutants (type I and II) with a deletion of MYR1, which blocks secretion of GRAs beyond the PV, yielded a non-significant impact on transmigration frequencies (Figure 1E; Supplementary Figures 1B, C). TgWIP and MYR1 deletion in type I parasites decreased DC motility on endothelium, in contrast with TgWIP deletion in type II parasites (Figure 1F). We conclude that parasite genotype-

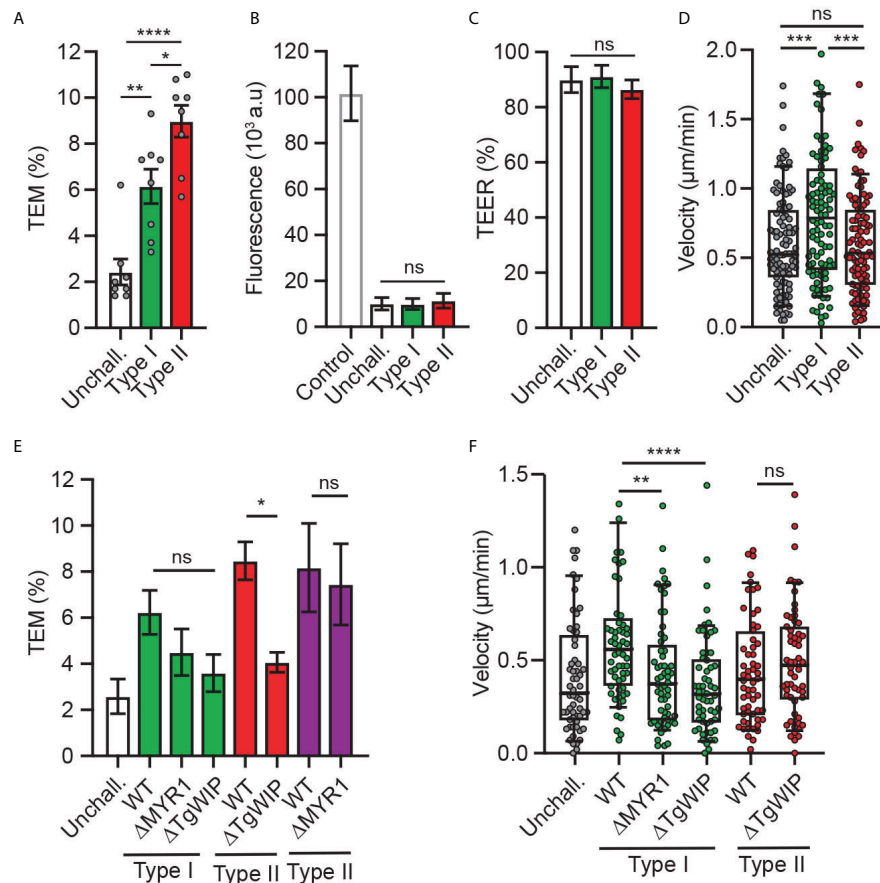


FIGURE 1

Transmigration and motility of *T. gondii*-challenged DCs on bEnd.3 monolayers. (A) Transendothelial migration (TEM) frequency of unchallenged or *T. gondii*-challenged (type I or II) DCs across bEnd.3 cell monolayers shown as percentage (%) of DCs added in the upper well. (B) Permeability of bEnd.3 monolayers to FITC-dextran (3 kDa) after DC TEM. Data are shown as arbitrary fluorescence units (a.u.) as specified under materials and methods. (C) TEER values of bEnd.3 cells relative to TEER values at initiation of the assay (100%). (D) Box-and-whisker and scattered dot plots represent median velocities ( $\mu\text{m}/\text{min}$ ) of unchallenged and *T. gondii*-challenged DCs on bEnd.3 monolayers. Each dot represents one tracked cell ( $n = 100$ ). (E) TEM frequencies of unchallenged DCs or DCs challenged with type I (RH; green bars) or type II (ME49-PTG; red bars, PRU; purple bars) WT or mutant strains across bEnd.3 cell monolayers shown as percentage (%) of DCs added in the upper well. (F) Box-and-whisker and scattered dot plots represent median velocities ( $\mu\text{m}/\text{min}$ ) of unchallenged and *T. gondii*-challenged DCs on bEnd.3 monolayers. Each dot represents one tracked cell ( $n = 60$ ). Bar graphs represent the mean  $\pm$  s.e.m of 3–4 independent experiments. \* $P < 0.05$ , \*\* $P < 0.01$ , \*\*\* $P < 0.001$ , \*\*\*\* $P < 0.0001$ , ns: non-significant, by one-way ANOVA, Sidak's *post-hoc* test.

related differences exist in the migratory activation of infected DCs and that both rhoptry-related secretion (TgWIP) and non-MYR1-associated effector(s) impact transmigration.

## ICAM-1 and integrin expression in *T. gondii*-challenged DCs

ICAM-1 and integrins were previously reported to play a role in the migratory phenotypes of *T. gondii*-infected DCs and monocytes, with an impact of antibody-blockade on TEM (24, 29). However, because ICAM-1 and integrins are expressed by both the endothelium and leukocytes (30), their precise roles in TEM

have remained unresolved. We therefore performed a detailed analysis of ICAM-1 and integrin expression in *T. gondii*-challenged DCs. We found that challenge of DCs with type II parasites induced elevated ICAM-1 transcription (Figure 2A). Consistently, flow cytometry analyses showed elevated ICAM-1 expression in type II-infected DCs but not in challenged non-infected DCs (Figure 2B), indicating absence of a by-stander effect. In contrast,  $\beta 1$  and  $\beta 2$  integrin expression remained essentially unchanged (Figure 2C), as previously described (24). Infection with type I parasites non-significantly impacted ICAM-1 expression in DCs (Figures 2A, B). Immunofluorescence intensity analyses corroborated elevated ICAM-1 signal in type II-infected DCs in absence of elevated signal in non-infected by-stander DCs or in type

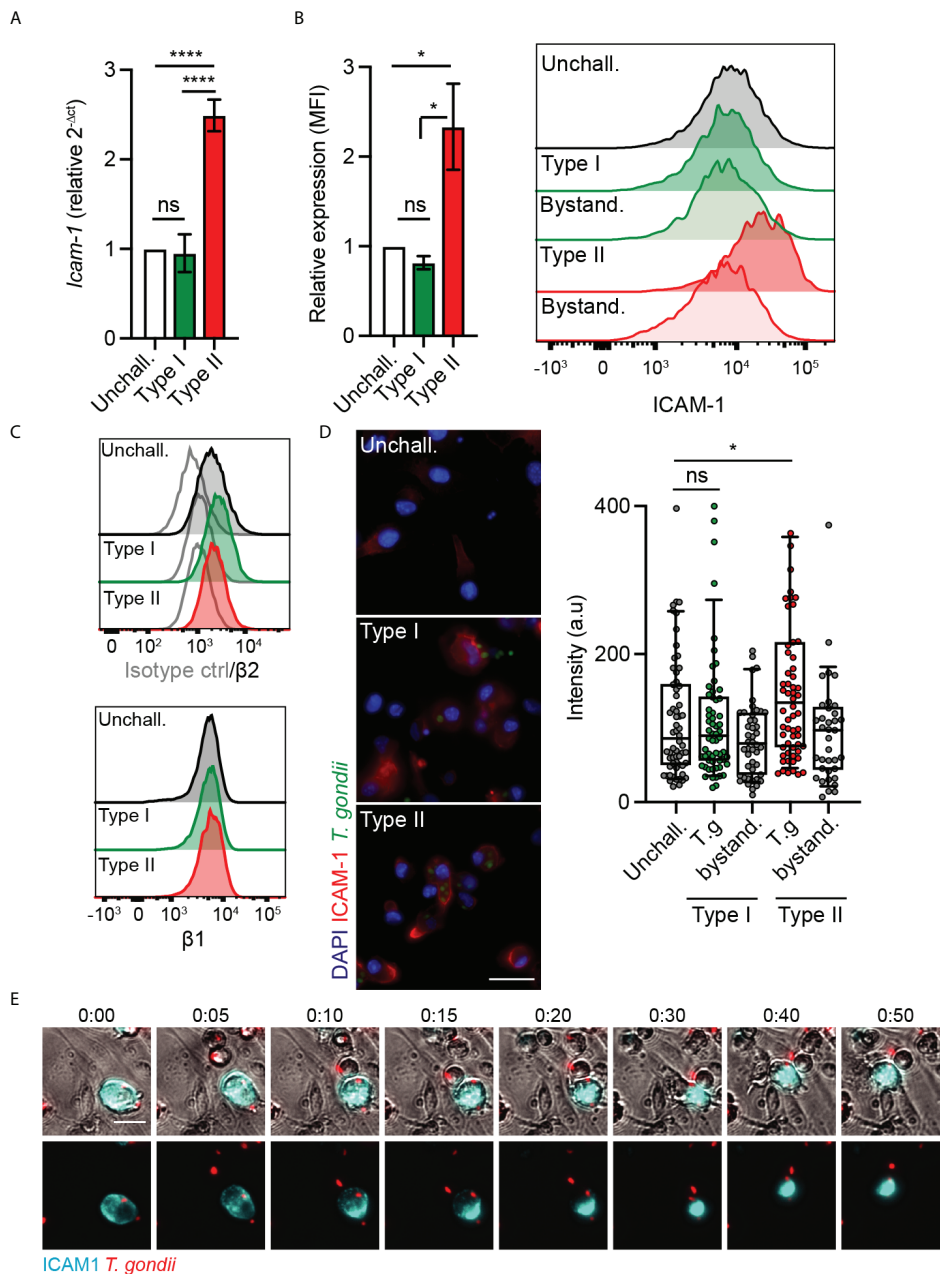


FIGURE 2

Parasite genotype-dependent upregulation and expression of ICAM-1 in DCs. (A) *Icam-1* mRNA expression ( $2^{-\Delta C_t}$ ) in DCs challenged with type I (RH) or II (ME49-PTG) *T. gondii* tachyzoites for 4 h, relative to unchallenged condition. (B) Bar graphs show relative expression of ICAM-1 (CD54) at 24 h post-challenge of CD11c<sup>+</sup> cells with *T. gondii* tachyzoites (GFP-expressing type I (RH) or type II (ME49-PTG), MOI 1), assessed by flow cytometry. Mean fluorescence intensity (MFI) was related to that of unchallenged CD11c<sup>+</sup> in complete medium (CM, normalised to 1). Histogram shows fluorescence intensity distributions for indicated cell populations. (C) Histograms show fluorescence intensity distributions of  $\beta 2$ ,  $\beta 1$  integrin and isotype antibody control for indicated cell populations, respectively, and are representative of 3 independent experiments. (D) Micrographs represent DCs infected with GFP-expressing *T. gondii* type I (RH) or II (ME49-PTG) (green) and stained for ICAM-1 (red) and nuclei (blue). Box-and-whisker and scattered dot plots show the corrected intensity fluorescence of one cell (n = 40–62), as detailed in materials and methods. (E) Representative micrographs of live cell imaging of type II (ME49) *T. gondii*-challenged DCs stained with anti-ICAM-1 APC antibody, on bEnd.3 cell monolayers. Scale bar = 20  $\mu$ m. Bar graphs represent the mean  $\pm$  s.e.m. of 3–4 independent experiments. \* $P < 0.05$ , \*\*\*\*  $P < 0.0001$ , ns: non-significant, by one-way ANOVA, Sidak's *post-hoc* test.

I-infected DCs (Figure 2D). Jointly, this indicated effects linked to parasite infection and to parasite genotype. Moreover, in live cell assays, a redistribution of the ICAM-1 fluorescence signal to the trailing edge of infected DCs preceded and accompanied their migration on endothelial cell monolayers (Figure 2E). We conclude that challenge of DCs with type II *T. gondii* led to a higher expression of ICAM-1, with a redistribution of ICAM-1 upon migration of parasitised DCs on endothelium.

## Leukocyte ICAM-1 is implicated in the motility on endothelium and TEM of infected DCs in a parasite genotype-related fashion

To address the function of DC ICAM-1 in the motility and transmigration of parasitised DCs, we applied combined approaches. First, based on previous findings indicating an implication of CAMs in TEM under static conditions (24), we assessed the velocities and pathlengths of *T. gondii*-infected DCs on bEnd.3 monolayers under shear stress. We found that type I-challenged DCs had a tendency for elevated velocities and significantly elongated pathlengths compared with type II-challenged DCs or unchallenged DCs, in presence or absence of antibody blockade using ICAM-1 mAb (Figures 3A, B). However, one of several caveats of antibody blockade is that it presumably targets both endothelial and leukocyte ICAM-1. Next, to specifically assess the role of leukocyte ICAM-1, we gene silenced *Icam-1* in DCs. Cell suspensions with transduced primary DCs (30–40% eGFP<sup>+</sup>, Supplementary Figure 2) presented a reduction in *Icam-1* mRNA expression related to control shLuc-transduced DCs (Figure 3C). Importantly, *Icam-1* silencing significantly elevated velocities and pathlengths in type II-challenged DCs but not type I-challenged DCs (Figures 3D, E). Conversely, while transmigration frequencies of unchallenged and type I-challenged DCs were non-significantly affected (Figures 3F, G), the transmigration frequencies of type II-challenged DCs across endothelial monolayers were significantly decreased in shICAM-1-transduced DCs compared with mock- or shLuc-transduced DCs (Figure 3H). We conclude that gene silencing of ICAM-1 (*Icam-1*) significantly inhibits transmigration of type II-challenged DCs but not of type I-challenged DCs. Consistent with motility data under static conditions (Figure 1), the inferior velocities and pathlengths under shear stress by type II-challenged DCs are indicative of ICAM-1-dependent adherence and TEM, while these effects are minimal or non-significant in type I-challenged DCs.

## The parasite effector GRA15 impacts ICAM-1 expression, motility and TEM of parasitised DCs

The findings that ICAM-1 silencing impacted transmigration in type II-infected DCs but not in type I-infected DCs motivated a

search for putative effectors. Consistent with our phenotypical data, the dense granule protein GRA15 was suspected because it is inactive in the type I RH strain but active in type II strains (31), and its effects do not depend on the MYR translocon (23). To test whether GRA15 is involved in the type II-induced increased expression of ICAM-1, DCs were challenged with wild-type (WT) or GRA15-deficient ( $\Delta$ GRA15) *T. gondii* lines and the expression of ICAM-1 was assessed by flow cytometry. Consistent with previous findings (Figure 2), WT-challenged DCs elevated ICAM-1 expression compared with unchallenged DCs (Figure 4A). In sharp contrast, DCs challenged with  $\Delta$ GRA15 failed to elevate ICAM-1 expression (Figure 4A), while integrin expression was maintained (Figure 4B). Importantly, DCs challenged with  $\Delta$ GRA15 parasites presented elevated motility on endothelium (Figure 4C) and, conversely, reduced transmigration frequencies across polarised endothelium (Figures 4D–F). We conclude that the increased expression of ICAM-1 in *T. gondii* type II-infected DCs is GRA15-dependent. Jointly, the data show that GRA15 expression is associated with elevated ICAM-1 expression, reduced velocities on endothelium and elevated TEM frequencies.

## Discussion

The mechanisms of leukocyte diapedesis across endothelium, and specifically DC trafficking across the BBB, entail complex signalling cascades that classically involve endothelial ICAM-1 (32). The upregulated expression of leukocyte ICAM-1 in *T. gondii*-infected DCs, in the absence of a by-stander effect, motivated an assessment of putative roles in TEM.

We demonstrate a role for leukocyte ICAM-1 in the motility on endothelium and the transmigration across polarised cerebral endothelium of DCs infected with the predominant type II *T. gondii* strains. Importantly, transcriptional upregulation of *Icam-1* was accompanied by elevated expression of ICAM-1 in infected DCs but not in by-stander DCs, indicating direct effects of intracellular parasitisation. Moreover, cell adhesion, motility and TEM *in vitro* were modulated by DC ICAM-1 expression. Of note, *T. gondii* infection also upregulates ICAM-1 expression in endothelial cell monolayers and the brain microvasculature (17, 33, 34). Therefore, antibody-blockade studies have correctly assumed an inhibitory effect on endothelial ICAM-1 (24, 29, 35) and the putative role of leukocyte ICAM-1 has remained unaddressed. Thus, in addition to endothelial ICAM-1, the present findings reveal that leukocyte ICAM-1 is implicated in TEM of parasitised DCs (Figure 5).

We recently reported a role for leukocyte  $\beta$ 1/2 integrins in the TEM of parasitised DCs (24). A major binding partner for ICAM-1 is the  $\beta$ 2 integrin LFA-1 (5, 6) and microvascular endothelium also expresses integrins, including LFA-1 (36). Thus, both integrins and ICAM-1 on leukocytes may interact

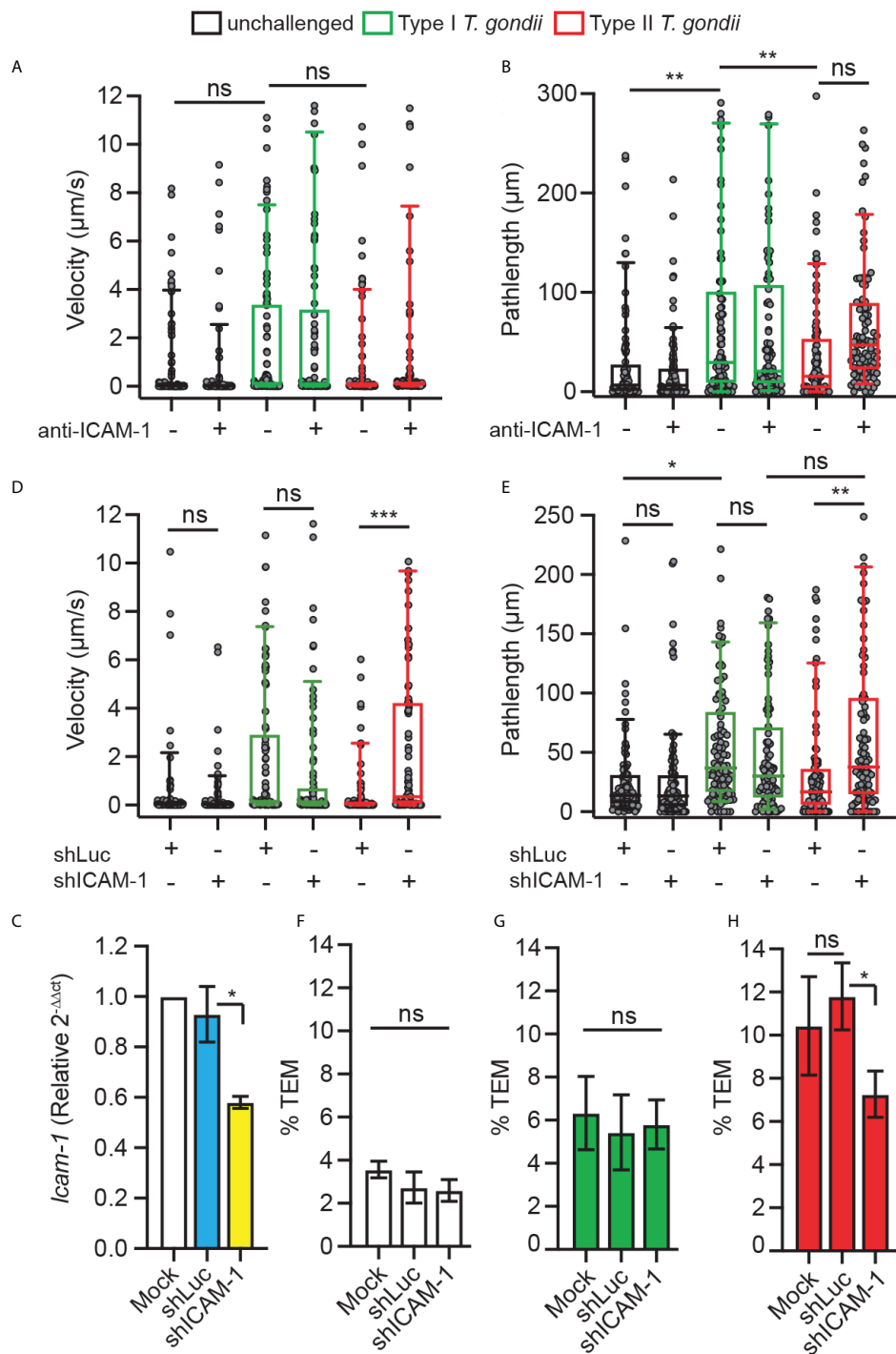


**FIGURE 3**

Implication of DC ICAM-1 in motility and TEM. (A, B) Box-and-whisker and scattered dot plots represent median velocities (µm/s) and pathlengths (µm), respectively, of type I (RH) or type II (ME49)-challenged DCs on bEnd.3 ± antibodies. Grey circles represent velocities or pathlengths, respectively, from individual cells. 95–100 cells were tracked per condition, from 3 independent experiments. (C) *Icam-1* mRNA expression (2<sup>-ΔΔCt</sup>) in DCs transduced with shICAM-1 or control shLuc lentivirus relative to mock-treated cells (mock set to 1.0). (D, E) Box-and-whisker and scattered dot plots represent median velocities (µm/s) and pathlengths (µm), respectively, of mock-treated DCs and DCs transduced with lentiviral vectors targeting *Icam-1* mRNA (shICAM-1) or a non-expressed target (shLuc) challenged with type I (RH) or II (ME49) *T. gondii* on bEnd.3. Grey circles represent velocities or pathlengths, respectively, from individual cells. 95–100 cells were tracked per condition, from 3 independent experiments. (F–H) TEM frequencies of unchallenged DCs (F), type I (RH)-challenged DCs (G) and type II (ME49)-challenged DCs (H) across bEnd.3 cell monolayers shown as percentage (%) of DCs added in the upper well. Bar graphs represent the mean ± s.e.m of 3–4 independent experiments. \**P* < 0.05, \*\**P* < 0.01, \*\*\**P* < 0.001, ns: non-significant, by one-way ANOVA, Sidak’s *post-hoc* test.

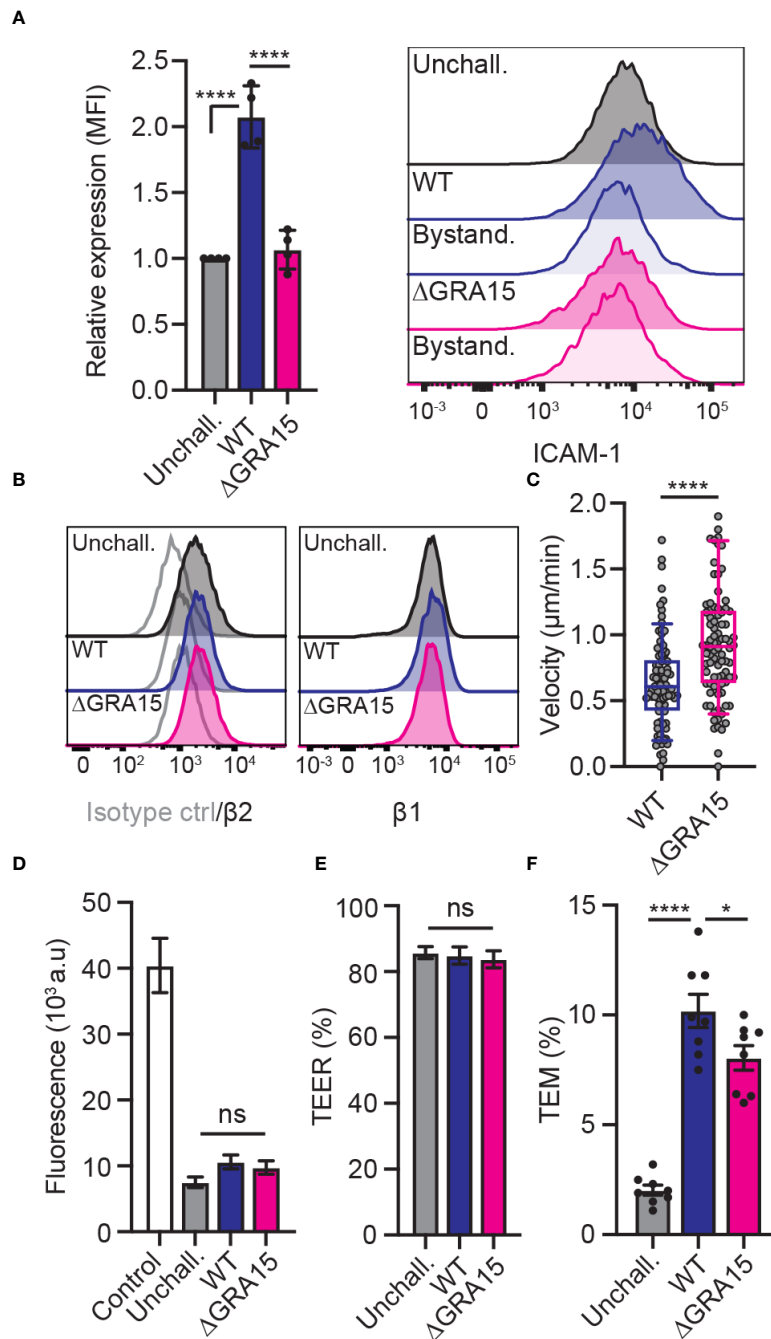


FIGURE 4

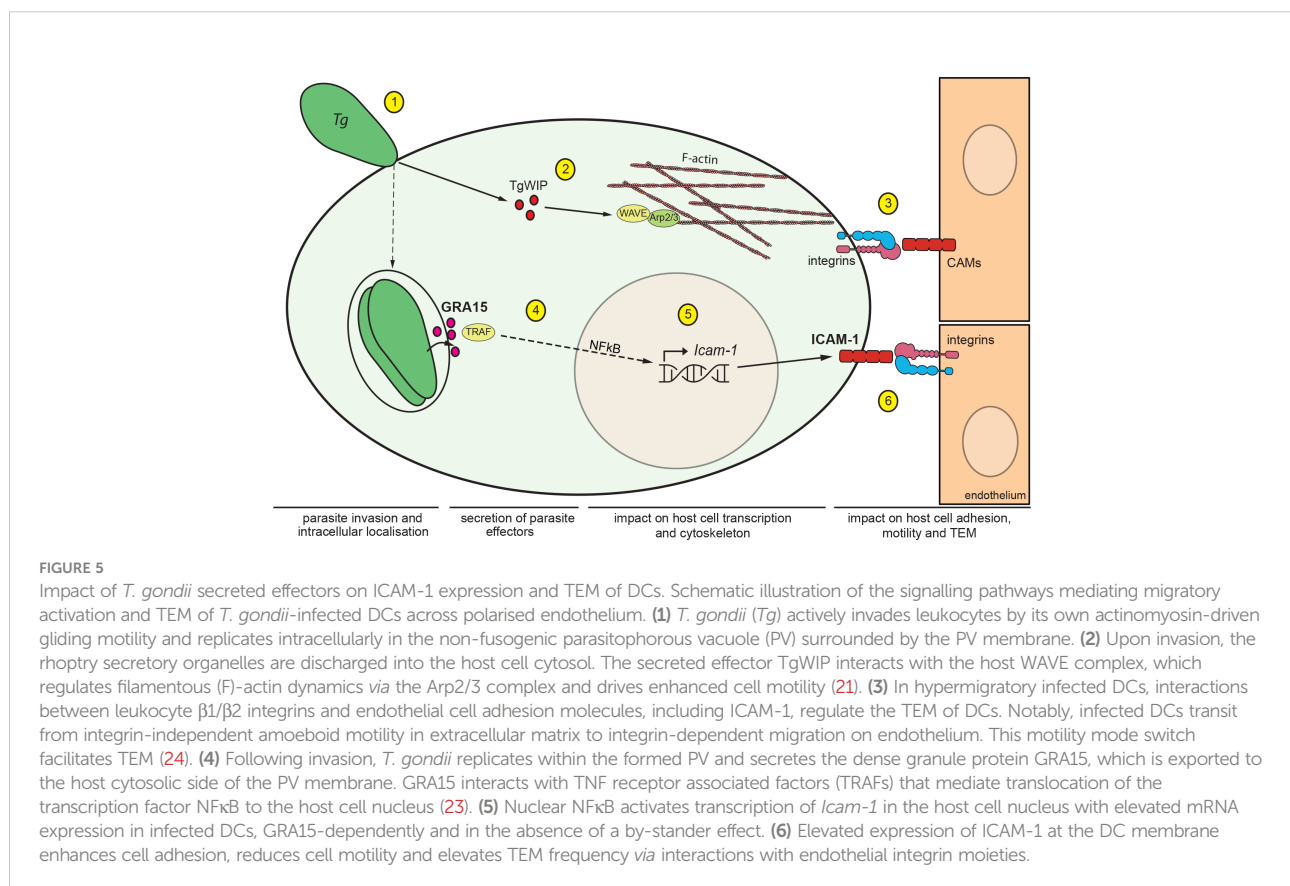
Impact of the effector GRA15 on ICAM-1 expression, motility and TEM of DCs. (A) Relative expression of ICAM-1 (CD54) at 24 h post-challenge of CD11c<sup>+</sup> cells with *T. gondii* tachyzoites (GFP-expressing PRU WT or PRU $\Delta$ GRA15, MOI 1), assessed by flow cytometry. Mean fluorescence intensity (MFI) was related to that of unchallenged CD11c<sup>+</sup> in complete medium (CM, normalised to 1). Histogram shows fluorescence intensity distributions for indicated cell populations. (B) Histograms show fluorescence intensity distributions of  $\beta$ 2,  $\beta$ 1 integrin and isotype antibody control for indicated cell populations, respectively, and are representative of 3 independent experiments. (C) Box-and-whisker and scattered dot plots represent median velocities of WT-challenged or  $\Delta$ GRA15-challenged DCs ( $\mu$ m/min). Grey circles represent velocities from individual cells. 90 cells were tracked per condition, from 3 independent experiments. (D) Permeability of bEnd.3 cell monolayers to FITC-dextran (3 kDa) following TEM of unchallenged, WT-challenged or  $\Delta$ GRA15-challenged DCs. (E) TEER values of bEnd.3 cells relative to TEER values at initiation of the assay (100%). (F) TEM frequencies of unchallenged, WT-challenged or  $\Delta$ GRA15-challenged DCs across bEnd.3 cell monolayers shown as percentage (%) of DCs added in the upper well. Bar graphs represent the mean  $\pm$  s.e.m of 4 independent experiments. \* $P$  < 0.05, \*\*\*\* $P$  < 0.0001, ns: non-significant, by one-way ANOVA followed by Sidak's *post-hoc* test (A, D, E, F) or Student's *t*-test (C).

with their corresponding moieties on endothelium, creating integrin-CAM interactions and, reciprocally, CAM-integrin interactions. The present study identifies leukocyte ICAM-1 as an additional determinant of DC transmigration *in vitro*. Along these lines, a critical role for ICAM-1 in mature DCs has been demonstrated for long-lasting contacts with CD8<sup>+</sup> T cells at the ‘immunological synapse’ (25). In contrast, ICAM-1 expression by neutrophils has been associated with phagocytosis and reactive oxygen species (ROS) responses but was not essential for transmigration (37). We provide proof-of-concept that leukocyte ICAM-1 can contribute to the TEM of DCs in the context of infection. Further studies need to address the contribution of ICAM-1 in other leukocytes, other inflammatory conditions and *in vivo* (7, 38).

The data suggest an implication of leukocyte ICAM-1 in the pathogenesis of toxoplasmosis. Interestingly, recent work reported that ICAM-1 is elevated in the cerebral microvasculature of mice challenged with *T. gondii* (17). Endothelial and epithelial ICAM-1 play pivotal roles in microbial pathogenesis, including the sequestration of *P. falciparum*-infected erythrocytes to endothelium in cerebral malaria (39), viral binding to epithelium (40) and bacterial invasion (41). Similarly, soluble ICAM-1 and ICAM-1 antibodies reduced the transmigration of extracellular *T.*

*gondii* tachyzoites across polarized epithelial monolayers (42). Thus, while the roles of endothelial and epithelial ICAM-1 in diapedesis are well established, the functions of leukocyte ICAM-1 have remained unelucidated in relation to microbial pathogenesis and diapedesis, including ICAM-1 isoform expression and function (43). Hypothetically, because the elevated expression of ICAM-1 in *T. gondii*-infected DCs is associated with endothelial adhesion, leukocyte ICAM-1 may contribute to mechano-transduction and therefore to TEM, as shown for endothelial ICAM-1 (44). Diapedesis encompasses tightly regulated cellular processes and signalling cascades. Thus, to promote its transportation in leukocytes, *T. gondii* needs to modulate cell adhesion, motility and TEM for efficient dissemination. Our data suggest that leukocyte ICAM-1 is targeted for these purposes.

We provide evidence that parasite effectors emanating from the dense granule and rhoptry secretory organelles, specifically GRA15 and TgWIP, are implicated in the enhanced TEM of parasitised DCs across endothelium (Figure 5). The data also provide a molecular framework for the previously observed parasite genotype-related differences in transmigration *in vitro* and dissemination in mice (45). Specifically, type II *T. gondii* strains relied to a higher extent than type I strains on transportation by DCs -Trojan horse mechanism- for systemic



dissemination (26). In line with the present findings, type II parasites also induced a stronger upregulation of ICAM-1 by brain endothelial cells, compared with type I parasites (34). Further, we extend previous findings that TgWIP significantly impacts the motility and TEM of parasitised DCs (21) to polarised endothelium. However, TEM was not totally abolished in DCs infected with TgWIP-deficient parasites. Jointly, this indicated the implication of additional genotype-related unidentified effector(s). Here, we report that secreted GRA15 (type II) impacts transcriptional upregulation of ICAM-1 and TEM. Moreover, the GRA15-related elevated expression of ICAM-1 was accompanied by elevated adhesion and reduction of motility of type II-challenged DCs on endothelium, consistent with impacts on the cellular processes of crawling, arrest and adhesion that precede transmigration (3, 4). In contrast, DCs challenged with type I parasites, which lack a functional GRA15 (23), failed to upregulate ICAM-1 and, contrary to type II infected DCs, increased motility on endothelium, suggesting reduced adhesion and therefore a reduced capability to transmigrate. Indeed, because GRA15 acts on the transcription factor NF $\kappa$ B (23) and ICAM-1 transcription requires the binding of NF $\kappa$ B (8, 46), it is reasonable to assume that this mechanism is in play. Thus, the concerted action of GRA15 and TgWIP seem to mediate the major part of the TEM phenotype for the type II strains tested (ME49, PRU). However, in the type I strain (RH) that lacks a functional GRA15 (47, 48), TgWIP-deficiency reduced but did not totally abolish TEM. This indicates that additional identified and unidentified effector(s) may contribute to TEM, including Tg14-3-3 (49) and the polymorphic effector ROP17 (50). Moreover, a cautious interpretation of phenotypes using prototypic strains is needed. For example, the lack of a functional version of the polymorphic effector GRA15 cannot be generalized to all type I strains (47, 48). Further, it cannot be ruled out that additional polymorphic and non-polymorphic effectors impact the ICAM-1-related migratory processes in a strain-related fashion. For example, ROP18 in type I (RH) has been shown to inhibit the host NF- $\kappa$ B pathway (51), which could further explain the reduced expression of ICAM-1. Moreover, the traits need to be confirmed *in vivo* in future studies despite the challenges that tracking infected leukocytes represent (12, 17).

The implication of several putative parasite effectors in TEM is consonant with the complexity of the hypermigratory phenotype induced by *T. gondii* in infected mononuclear phagocytes, including DCs, monocytes, macrophages and microglia (15, 52, 53). Indeed, several central functions of leukocytes, such as cell locomotion, adhesion, chemotaxis and ability to transmigrate, are modulated by *T. gondii*. Previous work demonstrated that dramatic and rapid changes take place in parasitised phagocytes shortly after *T. gondii* infection, encompassing cytoskeletal remodelling, dissolution of adhesive podosomes, redistribution of integrins and modulation of

extracellular matrix proteolysis (54–58). This implies the activation of several signalling pathways in the host cell (59), some of which are in response to the cellular environment and directly linked to integrin function (58, 60). Specifically, infected DCs transition between a high-speed integrin-independent amoeboid motility mode in extracellular matrix to an integrin-dependent motility mode on endothelium (24, 56). Here, we add the contribution of GRA15 to TEM through the induction of ICAM-1 expression in parasitized DCs. Of note, we previously found that treatment with LPS also upregulates ICAM-1 in DCs (24). However, LPS treatment does not induce hypermigration in DCs or other phagocytes (15, 61), indicating that ICAM-1 upregulation *per se* is not sufficient to induce the elevated TEM. We postulate that the concerted action of secreted polymorphic and non-polymorphic effectors mediates a migratory activation with modulated integrin function (24, 58, 60) and ICAM-1 expression in parasitised leukocytes, with an impact on the processes of TEM. Also, because the expression of cerebral endothelial E-selectin and VCAM-1 is modulated by *T. gondii* infection in mice (17), future studies need to determine their contribution to TEM.

The present work provides novel insights in how *T. gondii* orchestrates the modulation of host cell adhesion, motility and transmigration of parasitised leukocytes across polarised endothelium. While leukocytes facilitate the systemic dissemination of *T. gondii* (15, 16), their roles in mediating access to the brain parenchyma remain to be investigated (12). The infection of leukocytes by *T. gondii* may serve dual effects. The host leukocyte represents a replicative niche where the parasite is protected from immune attack in the PV, while transportation of intracellularly located parasites in migratory leukocytes facilitates dissemination.

## Data availability statement

The original contributions presented in the study are included in the article/[supplementary material](#). Further inquiries can be directed to the corresponding author.

## Ethics statement

The animal study was reviewed and approved by The Regional Animal Research Ethical Board, Stockholm, Sweden.

## Author contributions

ER and AH performed experiments and analysed the data. JS provided valuable reagents. All authors contributed to the writing of this manuscript.

## Funding

This work was funded by the Swedish Research Council (Vetenskapsrådet, 2018–02411) and the Olle Engkvist Foundation (193–609).

## Acknowledgments

We thank Dr. Manuel Varas-Godoy, San Sebastian University, Chile, for expert advice on lentiviral transduction.

## Conflict of interest

The authors declare that the research was conducted in the absence of any commercial or financial relationships that could be construed as a potential conflict of interest.

## Publisher's note

All claims expressed in this article are solely those of the authors and do not necessarily represent those of their affiliated organizations, or those of the publisher, the editors and the

reviewers. Any product that may be evaluated in this article, or claim that may be made by its manufacturer, is not guaranteed or endorsed by the publisher.

## Supplementary material

The Supplementary Material for this article can be found online at: <https://www.frontiersin.org/articles/10.3389/fimmu.2022.950914/full#supplementary-material>.

### SUPPLEMENTARY FIGURE 1

Infection frequency and assessments of polarisation and barrier integrity for transmigration assays. (A) Infection frequency of DCs challenged with type I or type II *T. gondii* at MOI 2 for 4 h. (B) TEER values of bEnd.3 cells relative to TEER values at initiation of the assay (100%), in . (C) Permeability of bEnd.3 cell monolayers to FITC-dextran (3 kDa) following TEM in . (D) Relative expression of ICAM-1 (CD54) at 24 h post-challenge of CD11c<sup>+</sup> cells with type II (PRU) *T. gondii* tachyzoites (WT or ΔMYR1, MOI 1), assessed by flow cytometry. Mean fluorescence intensity (MFI) was related to that of unchallenged CD11c<sup>+</sup> in complete medium (CM, normalised to 1). Bar graphs represent the mean ± s.e.m of 3–4 independent experiments. ns: non-significant, by one-way ANOVA, Sidak's post-hoc test.

### SUPPLEMENTARY FIGURE 2

Transduction of primary DCs. Representative micrographs of mock-treated DCs (Mock) and eGFP-expressing DCs transduced with shLuc or shICAM-1, as described in materials and methods. Transduction efficiency was consistently 30–40% based on eGFP expression. Scale bar = 100µm.

## References

- Abbott NJ, Ronnback L, Hansson E. Astrocyte-endothelial interactions at the blood-brain barrier. *Nat Rev Neurosci* (2006) 7(1):41–53. doi: 10.1038/nrn1824
- Klein RS, Hunter CA. Protective and pathological immunity during central nervous system infections. *Immunity* (2017) 46(6):891–909. doi: 10.1016/j.immuni.2017.06.012
- Ley K, Laudanna C, Cybulsky MI, Nourshargh S. Getting to the site of inflammation: the leukocyte adhesion cascade updated. *Nat Rev Immunol* (2007) 7(9):678–89. doi: 10.1038/nri2156
- Muller WA. Transendothelial migration: unifying principles from the endothelial perspective. *Immunol Rev* (2016) 273(1):61–75. doi: 10.1111/imr.12443
- Mamdouh Z, Mikhailov A, Muller WA. Transcellular migration of leukocytes is mediated by the endothelial lateral border recycling compartment. *J Exp Med* (2009) 206(12):2795–808. doi: 10.1084/jem.20082745
- Shaw SK, Ma S, Kim MB, Rao RM, Hartman CU, Froio RM, et al. Coordinated redistribution of leukocyte I $\alpha$ -1 and endothelial cell icam-1 accompany neutrophil transmigration. *J Exp Med* (2004) 200(12):1571–80. doi: 10.1084/jem.20040965
- Lyck R, Enzmann G. The physiological roles of icam-1 and icam-2 in neutrophil migration into tissues. *Curr Opin Hematol* (2015) 22(1):53–9. doi: 10.1097/MOH.0000000000000103
- Singh M, Thakur M, Mishra M, Yadav M, Vibhuti R, Menon AM, et al. Gene regulation of intracellular adhesion molecule-1 (icam-1): a molecule with multiple functions. *Immunol Lett* (2021) 240:123–36. doi: 10.1016/j.imlet.2021.10.007
- Pappas G, Roussos N, Falagas ME. Toxoplasmosis snapshots: global status of toxoplasma gondii seroprevalence and implications for pregnancy and congenital toxoplasmosis. *Int J Parasitol* (2009) 39(12):1385–94. doi: 10.1016/j.ijpara.2009.04.003
- Montoya JG, Liesenfeld O. Toxoplasmosis. *Lancet* (2004) 363(9425):1965–76. doi: 10.1016/S0140-6736(04)16412-X
- Schluter D, Barragan A. Advances and challenges in understanding cerebral toxoplasmosis. *Front Immunol* (2019) 10:242. doi: 10.3389/fimmu.2019.00242
- Ross EC, Olivera GC, Barragan A. Early passage of toxoplasma gondii across the blood-brain barrier. *Trends Parasitol* (2022) 38:450–61. doi: 10.1016/j.pt.2022.02.003
- Sibley LD, Ajioka JW. Population structure of toxoplasma gondii: clonal expansion driven by infrequent recombination and selective sweeps. *Annu Rev Microbiol* (2008) 62:329–51. doi: 10.1146/annurev.micro.62.081307.162925
- Fernandez-Escobar M, Schares G, Maksimov P, Joeres M, Ortega-Mora LM, Calero-Bernal R. Toxoplasma gondii genotyping: a closer look into europe. *Front Cell Infect Microbiol* (2022) 12:842595. doi: 10.3389/fcimb.2022.842595
- Lambert H, Hitziger N, Dellacasa I, Svensson M, Barragan A. Induction of dendritic cell migration upon toxoplasma gondii infection potentiates parasite dissemination. *Cell Microbiol* (2006) 8(10):1611–23. doi: 10.1111/j.1462-5822.2006.00735.x
- Courret N, Darche S, Sonigo P, Milon G, Buzoni-Gatel D, Tardieux I. Cd11c- and Cd11b-expressing mouse leukocytes transport single toxoplasma gondii tachyzoites to the brain. *Blood* (2006) 107(1):309–16. doi: 10.1182/blood-2005-02-0666
- Olivera GC, Ross EC, Peuckert C, Barragan A. Blood-brain barrier-restricted translocation of toxoplasma gondii from cortical capillaries. *Elife* (2021) 10:e69182. doi: 10.7554/eLife.69182
- Matta SK, Rinkenberger N, Dunay IR, Sibley LD. Toxoplasma gondii infection and its implications within the central nervous system. *Nat Rev* (2021) 19(7):467–80. doi: 10.1038/s41579-021-00518-7
- Hakimi MA, Boudour A. Toxoplasma's ways of manipulating the host transcriptome via secreted effectors. *Curr Opin Microbiol* (2015) 26:24–31. doi: 10.1016/j.mib.2015.04.003
- Rastogi S, Cygan AM, Boothroyd JC. Translocation of effector proteins into host cells by toxoplasma gondii. *Curr Opin Microbiol* (2019) 52:130–8. doi: 10.1016/j.mib.2019.07.002
- Sangare LO, Olafsson EB, Wang Y, Yang N, Julien L, Camejo A, et al. In vivo crispr screen identifies tgwip as a toxoplasma modulator of dendritic cell migration. *Cell Host Microbe* (2019) 26(4):478–92.e8. doi: 10.1016/j.chom.2019.09.008

22. Franco M, Panas MW, Marino ND, Lee MC, Buchholz KR, Kelly FD, et al. A novel secreted protein, *myr1*, is central to toxoplasma's manipulation of host cells. *mBio* (2016) 7(1):e02231–15. doi: 10.1128/mBio.02231-15
23. Rosowski EE, Lu D, Julien L, Rodda L, Gaiser RA, Jensen KD, et al. Strain-specific activation of the nf-kappab pathway by *gra15*, a novel toxoplasma gondii dense granule protein. *J Exp Med* (2011) 208(1):195–212. doi: 10.1084/jem.20100717
24. Ross EC, Ten Hoeve AL, Barragan A. Integrin-dependent migratory switches regulate the translocation of toxoplasma-infected dendritic cells across brain endothelial monolayers. *Cell Mol Life Sci* (2021) 78(12):5197–212. doi: 10.1007/s00018-021-03858-y
25. Scholer A, Hugues S, Boissonnas A, Fetler L, Amigorena S. Intercellular adhesion molecule-1-dependent stable interactions between t cells and dendritic cells determine cd8+ t cell memory. *Immunity* (2008) 28(2):258–70. doi: 10.1016/j.immuni.2007.12.016
26. Lambert H, Vutova PP, Adams WC, Lore K, Barragan A. The toxoplasma gondii-shuttling function of dendritic cells is linked to the parasite genotype. *Infect Immun* (2009) 77(4):1679–88. doi: 10.1128/IAI.01289-08
27. Fuks JM, Arrighi RB, Weidner JM, Kumar Mendu S, Jin Z, Wallin RP, et al. Gabaergic signaling is linked to a hypermigratory phenotype in dendritic cells infected by toxoplasma gondii. *PLoS Pathog* (2012) 8(12):e1003051. doi: 10.1371/journal.ppat.1003051
28. Vestweber D. How leukocytes cross the vascular endothelium. *Nat Rev Immunol* (2015) 15(11):692–704. doi: 10.1038/nri3908
29. Ueno N, Harker KS, Clarke EV, McWhorter FY, Liu WF, Tenner AJ, et al. Real-time imaging of toxoplasma-infected human monocytes under fluidic shear stress reveals rapid translocation of intracellular parasites across endothelial barriers. *Cell Microbiol* (2014) 16(4):580–95. doi: 10.1111/cmi.12239
30. Real E, Kaiser A, Raposo G, Amara A, Nardin A, Trautmann A, et al. Immature dendritic cells (dcs) use chemokines and intercellular adhesion molecule (icam)-1, but not dc-specific icam-3-grabbing nonintegrin, to stimulate cd4+ t cells in the absence of exogenous antigen. *J Immunol* (2004) 173(1):50–60. doi: 10.4049/jimmunol.173.1.50
31. Mukhopadhyay D, Arranz-Solis D, Saeij JPJ. Influence of the host and parasite strain on the immune response during toxoplasma infection. *Front Cell Infect Microbiol* (2020) 10:580425. doi: 10.3389/fcimb.2020.580425
32. Sagar D, Foss C, El Baz R, Pomper MG, Khan ZK, Jain P. Mechanisms of dendritic cell trafficking across the blood-brain barrier. *J Neuroimmunol Pharmacol* (2012) 7(1):74–94. doi: 10.1007/s11481-011-9302-7
33. Taubert A, Krull M, Zahner H, Hermosilla C. Toxoplasma gondii and neospora caninum infections of bovine endothelial cells induce endothelial adhesion molecule gene transcription and subsequent pmn adhesion. *Vet Immunol Immunopathol* (2006) 112(3-4):272–83. doi: 10.1016/j.vetimm.2006.03.017
34. Lachenmaier SM, Deli MA, Meissner M, Liesenfeld O. Intracellular transport of toxoplasma gondii through the blood-brain barrier. *J Neuroimmunol* (2011) 232(1-2):119–30. doi: 10.1016/j.jneuroim.2010.10.029
35. Furtado JM, Bharadwaj AS, Ashander LM, Olivas A, Smith JR. Migration of toxoplasma gondii-infected dendritic cells across human retinal vascular endothelium. *Invest Ophthalmol Vis Sci* (2012) 53(11):6856–62. doi: 10.1167/iov.12-10384
36. Klein S, Giancotti FG, Presta M, Albelda SM, Buck CA, Rifkin DB. Basic fibroblast growth factor modulates integrin expression in microvascular endothelial cells. *Mol Biol Cell* (1993) 4(10):973–82. doi: 10.1091/mbc.4.10.973
37. Woodfin A, Beyrau M, Voisin MB, Ma B, Whiteford JR, Hordijk PL, et al. Icam-1-expressing neutrophils exhibit enhanced effector functions in murine models of endotoxemia. *Blood* (2016) 127(7):898–907. doi: 10.1182/blood-2015-08-664995
38. Unno A, Kitoh K, Takashima Y. Up-regulation of hyaluronan receptors in toxoplasma gondii-infected monocytic cells. *Biochem Biophys Res Commun* (2010) 391(1):477–80. doi: 10.1016/j.bbrc.2009.11.083
39. Berendt AR, McDowall A, Craig AG, Bates PA, Sternberg MJ, Marsh K, et al. The binding site on icam-1 for plasmodium falciparum-infected erythrocytes overlaps, but is distinct from, the lfa-1-binding site. *Cell* (1992) 68(1):71–81. doi: 10.1016/0092-8674(92)90207-s
40. Staunton DE, Merluzzi VJ, Rothlein R, Barton R, Marlin SD, Springer TA. A cell adhesion molecule, icam-1, is the major surface receptor for rhinoviruses. *Cell* (1989) 56(5):849–53. doi: 10.1016/0092-8674(89)90689-2
41. Bhalla K, Chugh M, Mehrotra S, Rathore S, Tousif S, Prakash Dwivedi V, et al. Host icams play a role in cell invasion by mycobacterium tuberculosis and plasmodium falciparum. *Nat Commun* (2015) 6:6049. doi: 10.1038/ncomms7049
42. Barragan A, Brossier F, Sibley LD. Trans epithelial migration of toxoplasma gondii involves an interaction of intercellular adhesion molecule 1 (icam-1) with the parasite adhesin mic2. *Cell Microbiol* (2005) 7(4):561–8. doi: 10.1111/j.1462-5822.2005.00486.x
43. Ramos TN, Bullard DC, Barnum SR. Icam-1: isoforms and phenotypes. *J Immunol* (2014) 192(10):4469–74. doi: 10.4049/jimmunol.1400135
44. Schaefer A, Hordijk PL. Cell-stiffness-induced mechanosignaling - a key driver of leukocyte transendothelial migration. *J Cell Sci* (2015) 128(13):2221–30. doi: 10.1242/jcs.163055
45. Hitziger N, Dellacasa I, Albiger B, Barragan A. Dissemination of toxoplasma gondii to immunoprivileged organs and role of toll/interleukin-1 receptor signalling for host resistance assessed by in vivo bioluminescence imaging. *Cell Microbiol* (2005) 7(6):837–48. doi: 10.1111/j.1462-5822.2005.00517.x
46. Wissink S, van de Stolpe A, Caldenhoven E, Koenderman L, van der Saag PT. Nf-kappa B/Rel family members regulating the icam-1 promoter in monocytic thp-1 cells. *Immunobiology* (1997) 198(1-3):50–64. doi: 10.1016/s0171-2985(97)80026-5
47. Khan A, Behnke MS, Dunay IR, White MW, Sibley LD. Phenotypic and gene expression changes among clonal type i strains of toxoplasma gondii. *Eukaryotic Cell* (2009) 8(12):1828–36. doi: 10.1128/EC.00150-09
48. Yang N, Farrell A, Nieldelman W, Melo M, Lu D, Julien L, et al. Genetic basis for phenotypic differences between different toxoplasma gondii type i strains. *BMC Genomics* (2013) 14:467. doi: 10.1186/1471-2164-14-467
49. Weidner JM, Kanatani S, Uchtenhagen H, Varas-Godoy M, Schulte T, Engelberg K, et al. Migratory activation of parasitized dendritic cells by the protozoan toxoplasma gondii 14-3-3 protein. *Cell Microbiol* (2016) 18:1537–50. doi: 10.1111/cmi.12595
50. Drewry LL, Jones NG, Wang Q, Onken MD, Miller MJ, Sibley LD. The secreted kinase rop17 promotes toxoplasma gondii dissemination by hijacking monocyte tissue migration. *Nat Microbiol* (2019) 4(11):1951–63. doi: 10.1038/s41564-019-0504-8
51. Du J, An R, Chen L, Shen Y, Chen Y, Cheng L, et al. Toxoplasma gondii virulence factor rop18 inhibits the host nf-kappab pathway by promoting p65 degradation. *J Biol Chem* (2014) 289(18):12578–92. doi: 10.1074/jbc.M113.544718
52. Bhandage AK, Olivera GC, Kanatani S, Thompson E, Lore K, Varas-Godoy M, et al. A motogenic gabaergic system of mononuclear phagocytes facilitates dissemination of coccidian parasites. *Elife* (2020) 9:e60528. doi: 10.7554/Elife.60528
53. Weidner JM, Barragan A. Tightly regulated migratory subversion of immune cells promotes the dissemination of toxoplasma gondii. *Int J Parasitol* (2014) 44(2):85–90. doi: 10.1016/j.ijpara.2013.09.006
54. Olafsson EB, Varas-Godoy M, Barragan A. Toxoplasma gondii infection shifts dendritic cells into an amoeboid rapid migration mode encompassing podosome dissolution, secretion of timp-1, and reduced proteolysis of extracellular matrix. *Cell Microbiol* (2018) 20(3):e12808. doi: 10.1111/cmi.12808
55. Weidner JM, Kanatani S, Hernandez-Castaneda MA, Fuks JM, Rethi B, Wallin RP, et al. Rapid cytoskeleton remodeling in dendritic cells following invasion by toxoplasma gondii coincides with the onset of a hypermigratory phenotype. *Cell Microbiol* (2013) 15(10):1735–52. doi: 10.1111/cmi.12145
56. Kanatani S, Uhlen P, Barragan A. Infection by toxoplasma gondii induces amoeboid-like migration of dendritic cells in a three-dimensional collagen matrix. *PLoS One* (2015) 10(9):e0139104. doi: 10.1371/journal.pone.0139104
57. Olafsson EB, Ten Hoeve AL, Li-Wang X, Westermarck L, Varas-Godoy M, Barragan A. Convergent met and voltage-gated ca(2+) channel signaling drives hypermigration of toxoplasma-infected dendritic cells. *J Cell Sci* (2020) 134(5):jcs241752. doi: 10.1242/jcs.241752
58. Olafsson EB, Ross EC, Varas-Godoy M, Barragan A. Timp-1 promotes hypermigration of toxoplasma-infected primary dendritic cells Via Cd63-Itgb1-Fak signaling. *J Cell Sci* (2019) 132(3):jcs225193. doi: 10.1242/jcs.225193
59. Olafsson EB, Barragan A. The unicellular eukaryotic parasite toxoplasma gondii hijacks the migration machinery of mononuclear phagocytes to promote its dissemination. *Biol Cell* (2020) 112(9):239–50. doi: 10.1111/boc.202000005
60. Cook JH, Ueno N, Lodoen MB. Toxoplasma gondii disrupts Beta1 integrin signaling and focal adhesion formation during monocyte hypermotility. *J Biol Chem* (2018) 293:3374–85. doi: 10.1074/jbc.M117.793281
61. Lambert H, Dellacasa-Lindberg I, Barragan A. Migratory responses of leukocytes infected with toxoplasma gondii. *Microbes Infect/Institut Pasteur* (2011) 13(1):96–102. doi: 10.1016/j.micinf.2010.10.002